Experimental Brain Research (2019) 237:611–623
https://doi.org/10.1007/s00221-018-5442-9

RESEARCH ARTICLE

Impact of extremely low-frequency magnetic fields on human postural control

Sebastien Villard[1,2,3] · Alicia Allen[3] · Nicolas Bouisset[3] · Michael Corbacio[1] · Alex Thomas[1] · Michel Guerraz[4] · Alexandre Legros[1,2,3,5]

Received: 15 June 2018 / Accepted: 21 November 2018 / Published online: 5 December 2018

Abstract

Studies have found that extremely low-frequency (ELF, < 300 Hz) magnetic fields (MF) can modulate standing balance; however, the acute balance effects of high flux densities in this frequency range have not been systematically investigated yet. This study explores acute human standing balance responses of 22 participants exposed to magnetic induction at 50 and 100 mTrms (MF), and to 1.5 mA alternating currents (AC). The center of pressure displacement (COP) was collected and analyzed to investigate postural modulation. The path length, the area, the velocity, the power spectrum in low (< 0.5 Hz) and medium (0.5–2 Hz) bands have computed and showed the expected effect of the positive control direct current (DC) electric stimulation but failed to show any significant effect of the time-varying stimulations (AC and MF). However, we showed a significant biased stabilization effect on postural data from the custom experimental apparatus employed in this work, which might have neutralized the hypothesized results.

Keywords ELF MF · Humans · Postural control · Acute effect

Abbreviations

AC	Alternative current
ANOVA	Analysis of variance
BPPV	Benign paroxysmal positional vertigo
COP	Center of pressure
DC	Direct current
E-fields	Electric field
ELF	Extremely low-frequency
GVS	Galvanic vestibular stimulation
HFB	High frequency band
ICES	International Committee on Electromagnetic Safety
ICNIRP	International Commission for Non-Ionizing Radiation Protection
IEEE	Institute of Electrical and Electronics Engineers
LFB	Low frequency band
MF	Magnetic field
MFB	Medium frequency band

✉ Alexandre Legros
Alexandre.Legros@sjhc.london.on.ca

[1] Lawson Health Research Institute, St. Joseph Hospital, London, ON, Canada

[2] Medical Biophysics, Western University, London, ON, Canada

[3] School of Kinesiology, Western University, London, ON, Canada

[4] Laboratoire de Psychologie et Neurocognition, Université Savoie Mont-Blanc, Chambéry, France

[5] EuroMov, Université de Montpellier, Montpellier, France

Introduction

Exposure to artificial magnetic fields (MFs) has become increasingly prominent over the last few decades in our modern societies. Besides natural sources such as the earth MF, which is essentially static, man-made sources of time-varying MF are ubiquitous wherever electricity is produced, transported or used. Since MFs result from moving electric charges, time-varying electric currents such as those from domestic electricity (50 and 60 Hz) are generating MF at the same frequencies. These so-called extremely low frequency (ELF < 300 Hz) MF have the property to induce electric fields (E-fields) and currents in exposed conductors. As a conductor, the human body is subject to induced electric fields from time-varying MF, which have the potential to thus modulate biological processes (Saunders and Jefferys

2002, 2007; Foster 2003; Jefferys et al. 2003). It therefore becomes critical from an occupational and public health perspective to appropriately characterize and understand the possible consequences of ELF MF exposures on human physiology and neurophysiology. Average levels of public exposure to ELF MF are between 0.01 and 1.0 μT over 24 h in North America (Rankin et al. 2002) with peak exposures as high as 0.3 mT (Mezei et al. 2006), which may be associated with certain electrical household appliances or equipment. For those working closely to high current conductors, such as live-line electric utility workers, exposure levels may reach up to 1–10 mT (Bracken et al. 2001; World Health Organization 2007). It is essential to establish if these exposure levels, to which one can be exposed for short or longer periods of time, potentially have biological or adverse health effects. This careful scientific review is conducted by international agencies such as the International Commission for Non Ionizing Radiation Protection (ICNIRP) and the International Committee on Electromagnetic Safety from the Institute of Electrical and Electronics Engineers (IEEE-ICES), which also publish guidelines and recommendations (IEEE 2002; International Commission on Non-Ionizing Radiation Protection 2010). Electrostimulation remains the only basis with known mechanisms for establishing guidelines and standards to protect against adverse effects, with magnetophosphenes and peripheral nerve stimulation defining the frequency characteristics of these exposure limits.

Magnetophosphenes are instantaneously occurring flickering visual perceptions when exposed to a magnetic field, first reported in 1896 (d'Arsonval 1896) and have been investigated since then (Barlow et al. 1947; Lövsund et al. 1980b; Attwell 2003). The threshold for perception of a magnetophosphene is affected by a number of factors (e.g., ambient lighting) including the frequency of the time-varying magnetic field (Barlow et al. 1947; Lövsund et al. 1980b) with the lowest thresholds occurring at about 20 Hz. It has been experimentally and theoretically suggested that magnetophosphenes are the result of a magnetic induction of E-field at the level of the retinal photoreceptors, likely the rods (Barlow et al. 1947; Attwell 2003). Attwell (2003) argued that the retina is the likely source for magnetophosphene perception because the morphology of the photoreceptors makes them particularly susceptible to induction mechanisms, but also because of the signal amplifying properties of the retina, which has been shown to be capable to detect a single photon (Tinsley et al. 2016). Such properties are enabled by different characteristics of the retina, but Attwell (2003) emphasized the role of the graded potential cells that allow continuous transmission of information through their ribbon synapses. The presence of graded potential cells in other sensory systems, such as the hair cells in the vestibular system (Eatock 2006 for review), calls into question whether other acute biological effects can be observed upon exposure to ELF MFs. For instance, one might suggest that modifications of information processing by hair cells would affect the vestibular function greatly involved in postural control.

Interestingly, previous research with human subjects has reported effects of ELF MFs on postural control during ELF MF exposure (Prato et al. 2001; Thomas et al. 2001a, b; Legros et al. 2012; van Nierop et al. 2013; van Nierop 2015). The control of posture is enabled by the integration of information gathered by the visual, auditory, sensory-motor, and vestibular systems (Magnusson et al. 1990; Bronstein and Guerraz 1999; Stål et al. 2003). The vestibular system is of particular interest since it is responsible for controlling gaze stabilization and maintaining the position of the head regarding the rest of the body, and therefore controlling the overall balance (Cullen 2012). However, the results of studies addressing the potential impact of ELF MFs on postural control and the vestibular system remain inconsistent. For example, some studies show a stabilization effect with respect to time-varying MF exposure (Thomas et al. 2001a, b; Legros et al. 2012; van Nierop 2015), some show a destabilization effect (Prato et al. 2001; van Nierop et al. 2013), and some show no effect at all (Glover et al. 2007). These studies all differ with respect to experimental design, making comparison of results among them difficult. Moreover, MF exposures on the order of those used in magnetophosphenes studies (Barlow et al. 1947; Lövsund et al. 1980b; Attwell 2003) (in the tens of mT) have not been investigated in the context of postural control.

An extensive body of work has been published on the effect of strong static fields on the vestibular system. Marcelli et al. (2009) first reported the existence of nystagmus in healthy participants exposed to a 1.5 T static field within an MRI system, suggesting that the vestibular system was stimulated by the static MF. Since then, this effect has been confirmed and hypothesized as the consequence of the Lorentz forces created by strong static magnetic field on the ionic currents present in the endolymph of the vestibular system (Roberts et al. 2011; Antunes et al. 2012; Glover et al. 2014; Ward et al. 2015; Otero-Millan et al. 2017). Over 1.5 T, these forces are considered sufficiently large to push the cupula within the semicircular canals (Otero-Millan et al. 2017).

A well-known methodology to stimulate the vestibular systems with current, called galvanic vestibular stimulation (GVS), induces changes in postural control (Fitzpatrick and Day 2004). This method consists of applying a direct current (DC-GVS) or alternating current (AC-GVS) stimulation at the level of the mastoid process. For DC-GVS, the result is a clear tilt towards the side of the anodal stimulation, while AC-GVS results in a smaller amplitude rhythmic side-by-side sway that decrease with frequency (Hlavacka and Njiokiktjien 1985). GVS is often described as

a depolarization of the vestibular afferents (Goldberg et al. 1984), however several studies suggest that the hair cells are not bypassed but rather directly stimulated by currents (Norris et al. 1998; Aw et al. 2008; Gensberger et al. 2016). It also important to note that both the otolith organs and the semicircular canals are stimulated by GVS (Curthoys and MacDougall 2012). It is broadly reported that the vestibular system is well-tuned to respond to one's natural motion. Recent studies have shown that natural motion frequencies in humans range from 0 to 30 Hz (Carriot et al. 2014). Furthermore, studies looking at myogenic responses showed that vestibular stimulation of up to 100 Hz can affect muscular activity (Forbes et al. 2013, 2014, 2016, 2018) which might help us understand previous experimental findings mentioned above showing postural modulation due to the interaction with time-varying magnetic fields (Prato et al. 2001; Thomas et al. 2001a, b; Legros et al. 2012; van Nierop et al. 2013; van Nierop 2015). Looking at the vestibular performance more closely, the latency of the vestibular ocular reflex is known to be around 6–7 ms (Cullen 2012 for review), which should enable vestibular system sensitivity to frequencies in the order of 160 Hz. Lastly, it is known that otolithic cells respond to stimulation above 1000 Hz (Curthoys et al. 2018 for review). Therefore, the vestibular system is most likely susceptible to MF exposure at the power frequencies of 50 or 60 Hz.

The main objective of this study was to determine whether exposure of the vestibular system to a 60-Hz MF triggers an acute postural response in humans. The second objective was to confirm the inductive origin of this effect by testing the response to AC-GVS given at the same frequencies delivering currents on the same order of magnitude. Different stimulus frequencies were used to evaluate whether the response is frequency dependent, as previously observed in magnetophosphenes studies (Lövsund et al. 1980a).

Materials and methods

Participants

Twenty-two healthy participants (12 males, 10 females, mean age: 23 ± 4.8) were tested in the Human Threshold Research Facility at St. Joseph's Hospital in London, Ontario, Canada. We excluded individuals with history of vestibular-related pathology (such as benign paroxysmal positional vertigo (BPPV), labyrinthitis or vestibular neuritis, Ménière's disease, secondary endolymphatic hydrops and perilymph fistula), chronic illnesses (including cardiovascular diseases, such as hypertension, ischemia, and cerebrovascular disease) and neurological diseases that affect normal body movement (such as Parkinson's disease or multiple sclerosis). We also excluded people under treatment for hypertension and people who are prone to seizures, self-reported permanent metal devices or piercings above the neck region or reported recreational drug use. Participants were asked to abstain from alcohol and caffeine intake for 24 h prior to the experiment. This protocol was approved by Western University's Ethics Board for Health Science Research Involving Human Subjects (protocol #106122).

Materials

A force plate (OR6-7-1000, AMTI, USA) was used to record the displacement of Center-Of-Pressure (COP) with a sampling rate of 10 kHz, using an A/D National Instrument card (NI SCB-68A, National Instruments, USA), driven by LabView 14.0.1 (National Instruments, USA). The LabView program collected forces and moments in the three dimensions, along with MF measurement time series.

The two modalities of electric stimulation, DC-GVS and AC-GVS, were delivered using the StarStim system (StarStim, Neuroelectrics, Spain–see Fig. 1, left panel), and time stamps were sent to the LabView program for synchronization purposes. Two Sponstim sponge electrodes were placed at F3 and F4 (positioned according to the standard international 10–20 system), and two Pistim Ag/AgCl electrodes were placed over the left and the right mastoid processes (M1 and M2, respectively). In the AC-GVS, the anode was placed over M1 and the return electrode over F4 for the left anodal stimulation condition. The anode was placed over M2 and the return electrode over F3 for the right anodal stimulation. This choice was made to allow a unilateral vestibular exposure. As the positive control condition, the DC-GVS exposure uses the standard bilateral electrode positioning. Anodal stimulation conditions on the left (M1) and on the right (M2) were delivered to maximize the effects. NIC (Neuroelectrics Instrument Controller, version 1.4.1 Rev.2014-12-01) software was used to drive the StarStim device via Bluetooth and force plate recordings were synchronized via timestamp. The MF exposure was delivered via a customized head set coil exposure system (Fig. 1, top right panel, and detailed diagram on bottom panel), consisting of two 570 turn coils of 5.9 cm of mean diameter. A 25.48 mm diameter core of Permendur-49 (The Goodfellow Group, Coraopolis, PA, USA) was used to increase the flux density developed by the coil to reach 100 mTrms at 3 cm from the coil. The inductances of the coils were 26 mH. The coils were attached to an adjustable helmet-like device to fit directly beside each mastoid process for an exposure targeting the vestibular system exposure. Because of the heavy weight of the apparatus (6.70 kg), a matching counterweight was attached to the helmet with a rope sliding through a pulley placed above the head of the tested volunteer. This apparatus allowed to position the helmet and the coils over the head of participants, without having to support

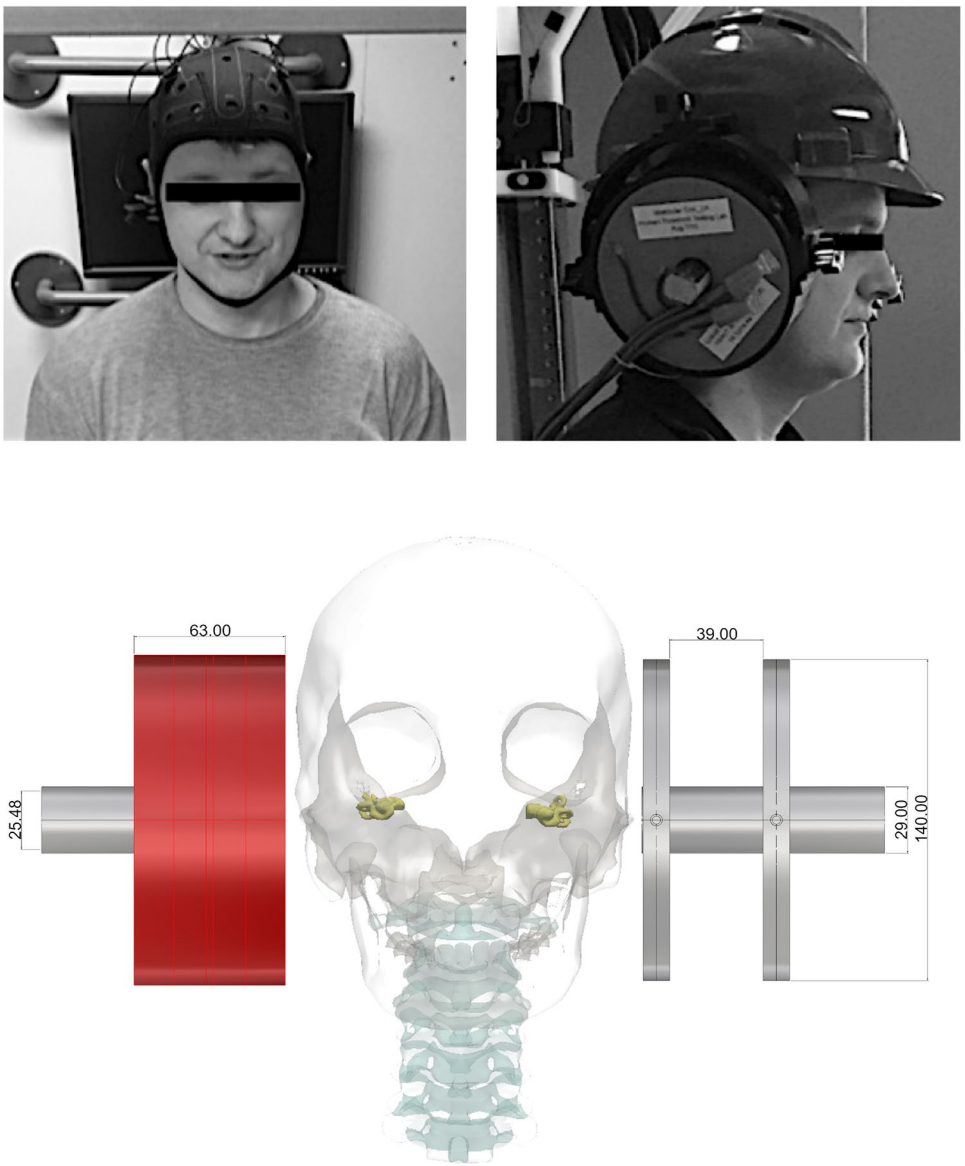

Fig. 1 Exposure apparatus. Volunteer wearing the cap of the Starstim device used for DC- and AC-GVS (top left panel) and the helmet supporting the coils for MF exposure (top right panel). The bottom panel represents a diagram of the coil system with outer casing measurements (in mm) on the left, and inner measurements where the wiring is setting to the right. A core of Permendur49 of 25.48 mm was placed at the center of each coil. The head depicted in between the coils shows the location of each vestibular system located at about 3 cm from the surface of each coil

the weight of the device, still allowing free movement of the subject's head and body. The stimulation waveform was generated with Labview 14.0.1 and sent to two MRI gradient amplifiers (MTS AUTOMATION, Model 0106475, USA) through the same A/D National Instrument module. Each amplifier drove one coil (Left or Right) to produce a MF of up to 100 mTrms at 3 cm from the coil surface. Figure 2 shows the measurements of MF flux densities recorded with single axis MF Hall transducer probe (±200 mTrms range with 0.1% accuracy, SenisTM 0YA05F-C.2T2K5J; Senis, Baar, Switzerland).

Experimental procedure

For each subject, the experiment consisted of a single study session lasting 2 h and 30 min. The initial 20 min were devoted to explaining the study and obtaining the subject's written consent to participate. The following 20 min were devoted to setting up the participant with the StarStim exposure device. Next, an impedance check was performed, and the participants were exposed to a short DC-GVS (1.5 mA) and AC-GVS (1.5 mA, 20 Hz) exposure as a familiarization sample before the actual testing took place. The actual testing sessions consisted of 33 randomized conditions, split up into 3 sub-sessions of 11 testing conditions each. Each session lasted approximately 25 min, with a 5-min break between sub-sessions allowing for the participant to rest.

Each testing condition consisted of approximately 30-s period of standing on the force plate. Participants were asked to stand still with their feet together, arms resting at their sides, and eyes closed. The force plate was covered with a fitness mat to minimize proprioceptive cues about

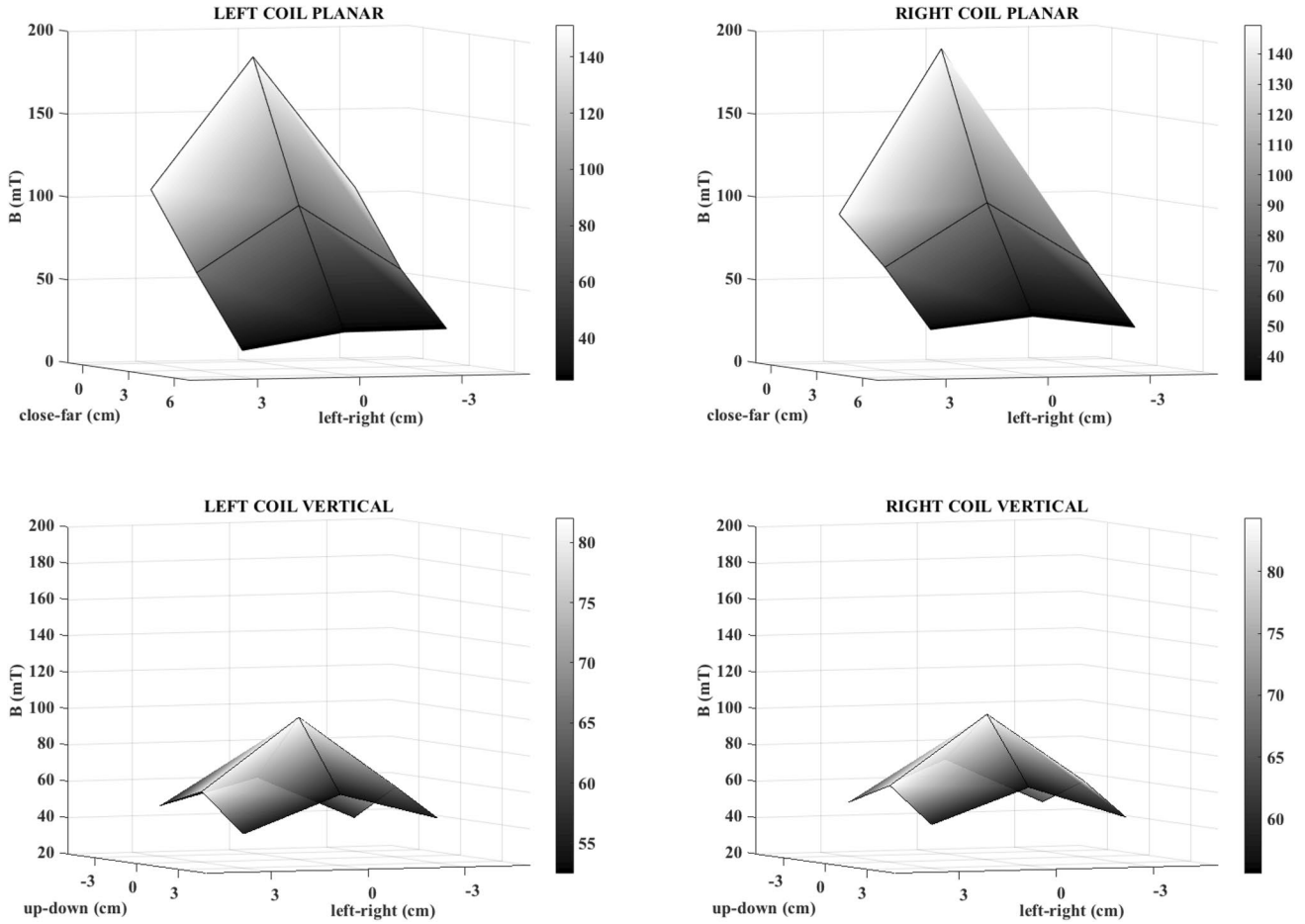

Fig. 2 Measurements of the flux density for a targeted 100 mTrms at 3 cm from the surface of the coil with core in the planar plane (top panels) and in the vertical plane (bottom panels)

body positioning. Participants wore earplugs to minimize any possible audio cues. For consistency, both the StarStim exposure cap and the MF exposure device were on the head during all testing conditions. After the participants were instructed to close their eyes at the onset of each condition, the data acquisition began with 10 s of baseline recording, followed by the 5 s of stimulation and ended 10 s after exposure. In the case of DC and AC-GVS, 2 s of ramp-up and ramp-down, respectively, before and after the actual 5 s of stimulation at 1.5 mA were used to minimize discomfort.

The 33 randomized exposures conditions consisted of 1 Sham exposure (no stimulation was applied), 2 DC-GVS 1.5 mA exposures (anode on each side of the head), 10 AC-GVS 1.5 mA exposures (5 anode left and 5 anode right with stimulation frequencies of interest at: 20, 60, 90, 120, or 160 Hz), and 20 MF exposures (5 same frequencies of interest applied on the left and on the right side of the head at 2 flux density levels: 50 mT and 100 mT). The choice of the frequencies of interest was based on the resting firing frequency of vestibular hair cells afferences reported to be 90 Hz in primates of similar size to humans (Goldberg et al. 2012). The rational was that a unilateral stimulation given at the resting firing frequency should have minimal to no impact of function, since it is unlikely to induce a differential rhythm between the left and right vestibular systems. Since it is the differential firing rates between the left and right vestibular that are interpreted as head accelerations in one direction or the other (i.e., perception of lateral acceleration), it was chosen to use two unilateral stimulation frequencies below and two above the resting frequency. The 20 Hz condition was selected because this is the optimal frequency for magnetophosphene perception (Lövsund et al. 1980b) and 60 Hz because it is the power frequency in North America. As frequencies below the 90 Hz mark, 20 Hz and 60 Hz should both induce similar effects possibly of different sizes. The 120 and 160 Hz conditions were selected as the symmetric frequencies 20 and 60 Hz above 90 Hz and were expected to induce effects in the opposite direction.

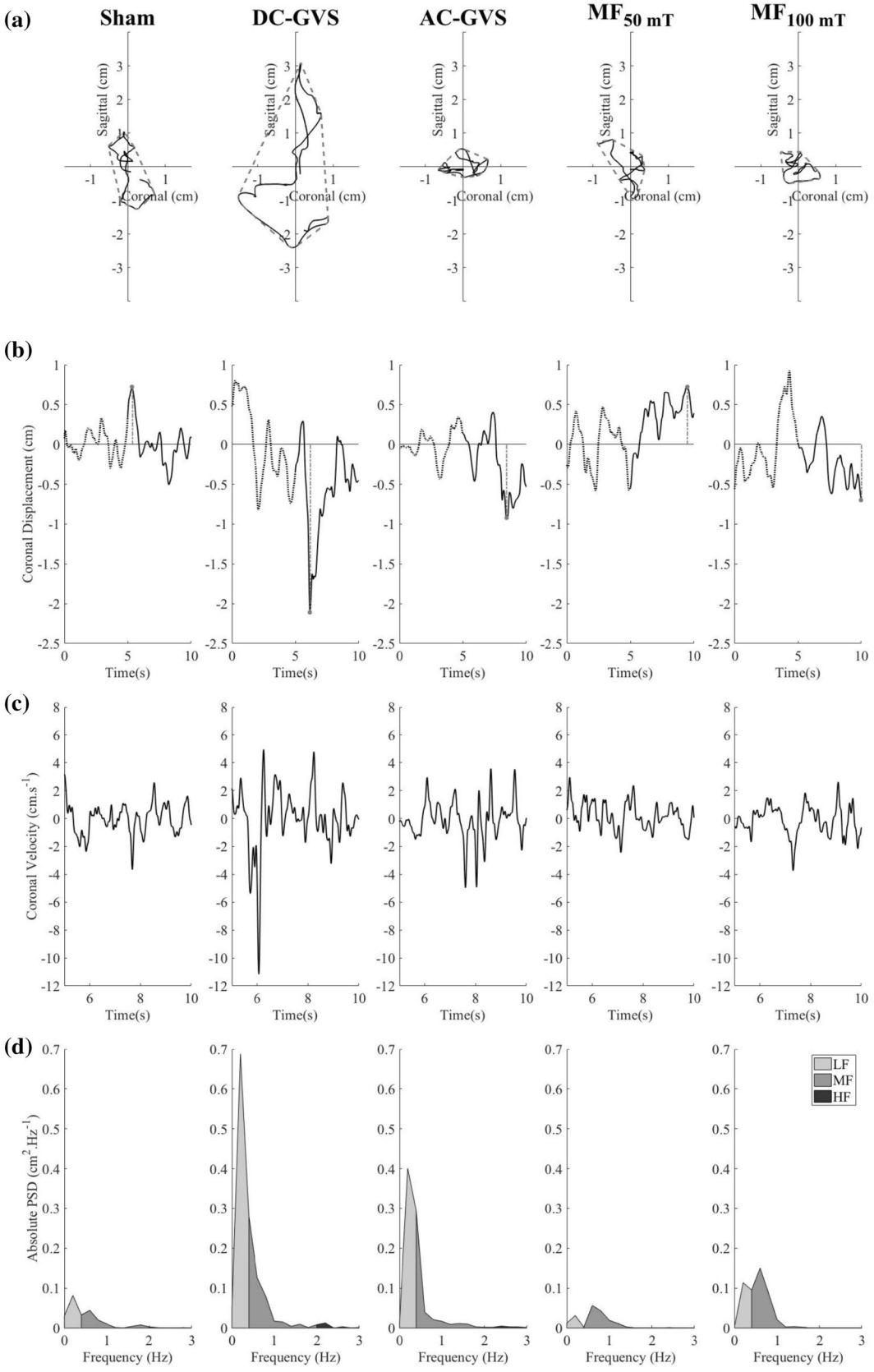
(a)
Sham
DC-GVS
AC-GVS
MF50 mT
MF100 mT
Sagittal (cm)
Coronal (cm)
(b)
Coronal Displacement (cm)
Time(s)
(c)
Coronal Velocity (cm.s-1)
Time(s)
(d)
Absolute PSD (cm2.Hz-1)
Frequency (Hz)
LF
MF
HF

◂**Fig. 3** COP data from participant #8 for the following 5 experimental conditions: Sham, DC-GVS, AC-GVS, MF50 mT, and MF100 mT (from left to right: all exposures administrated on the left side of the head and at 90 Hz for AC and MF stimulations, respectively). **a** Represent the sway path, and the area of the COP during exposure. **b** Represent the coronal displacement of the COP before exposure (dashed curve) and during exposure (solid curve). The straight lines represent the mean coronal position before (dashed line) and during (solid line) exposure. The lateral coronal displacement (gray arrows) was computed as the difference between the before and during average positions. **c** Represent the coronal velocity during exposure. **d** Represent the spectral density of the coronal position of the COP during exposure. Each frequency band is represented in a grayscale: the LFB (< 0.5 Hz), MFB (> 0.5 Hz, < 2 Hz), and HFB (> 2 Hz)

Variables and statistical analysis

The COP time series were low-pass filtered with a cutoff frequency of 10 Hz and analyzed using MatLab 9.0 (The MathWorks Inc., USA). The following sway characteristics were computed from the filtered COP data: path length (cm), sway area (cm^2), mean coronal velocity (cm/s), lateral coronal displacement (cm). The coronal time series were also analyzed in the frequency domain (See Fig. 3). Path length was calculated as the sum of the distance between each sequential point of measurement. Area was calculated as the total enclosed area of the participant's movement using the minimum enclosed polygonal area of the plotted outer vertices using Matlab's convex hull function (illustrated in Fig. 3, a panels, as dotted line around the COP displacement). Lateral coronal displacement was calculated as a difference between the average COP position of a 5 s period pre-exposure and the peak of center of pressure position over the 5 s period of exposure (Yang et al. 2015) (as illustrated in Fig. 3, panels b). A positive difference describes a displacement to the right and a negative difference describes displacement to the left. Coronal velocity was calculated as the mean of the absolute coronal displacement per sampling period (Fig. 3, c panels). The frequency domain analysis of coronal displacements consisted of Matlab computing the Welch's power spectral density estimate over 2.5 s Hamming windows with 1.25 s overlaps. This method was chosen to reduce the variability of the periodogram produced by a traditional fast Fourier transform. The spectral density (Fig. 3, d panels) informed us of the power of coronal oscillations per frequency. We distinguished three frequency bands as described by Paillard and Noé (2015): the low frequency band (LFB, < 0.5 Hz), the medium frequency band [MFB, (0.5–2) Hz], and the high frequency band (HFB, > 2 Hz). We computed the sum of power density over each frequency band. Since 99.01% of the spectrum density was observed below 2 Hz for all participants in all conditions, only the LF and MF were considered meaningful and were analyzed.

The statistical analysis consisted of three within-subject repeated measure ANOVAs. The first one-way ANOVA compared the experimental exposure effect including the Sham condition (five levels: Sham, DC-GVS, AC-GVS, MF_{50mT}, and MF_{100mT}). The second test explored the effect of side of exposure using a two by four ANOVA with the first factor being side of exposure (two levels: left and right), and the second factor being exposure (four levels: DC-GVS, AC-GVS, MF_{50mT}, and MF_{100mT}). Finally, the third analysis focused on the frequency of the different time-varying exposure types using a 3 × 2 × 5 ANOVA: exposure (three levels: AC-GVS, MF_{50mT} and MF_{100mT}) × side (two levels: left and right) × frequency (five levels: 20 Hz, 60 Hz, 90 Hz, 120 Hz and 160 Hz). R version 3.3.1 was used for all statistical analyses (R Core Team 2016).

Results

The five modalities (Sham, DC-GVS, AC-GVS, MF_{50mT}, and MF_{100mT}) in within-subjects one-way ANOVA showed that the path length was significantly modulated by the exposure condition ($F(4,84) = 10.91$, $p < 0.001$, Fig. 4). Tukey's honest significant difference (Tukey HSD) post hoc comparison showed that the path length was significantly higher during DC-GVS exposure than during any other stimulation (Sham, AC-GVS, MF_{50mT} and MF_{100mT} exposure). The same exposure effects were also found for area ($F(4,84) = 7.34$, $p < 0.001$), coronal velocity ($F(4,84) = 10.15$, $p < 0.001$), absolute spectral density in the LFB ($F(4,84) = 5.62$, $p < 0.001$), and in the MFB ($F(4,84) = 4.19$, $p < 0.01$).

No significant effects of exposure were found on the lateral coronal displacement.

The two (side: left, right) × 4 (exposure: DC-GVS, AC-GVS, MF_{50mT}, and MF_{100mT}) within-subjects ANOVA tested the effect of the exposure side, including the positive control (DC-GVS) but excluding the Sham condition given only once and already tested by the first ANOVA. First of all, the main exposure effect resulting from the significant DC-GVS effect over any other stimulation was found again on path length ($F(3,63) = 10.93$, $p < 0.001$), area ($F(3,63) = 7.84$, $p < 0.001$), and coronal velocity ($F(3,63) = 10.17$, $p < 0.001$), absolute spectral density in the LFB ($F(3,63) = 5.61$, $p < 0.01$) and the MFB ($F(3,63) = 4.19$, $p < 0.01$).

The lateral coronal displacement is particularly interesting here since it represents displacement towards one side of the body or the other. We found a significant interaction between experimental condition and the side of the stimulation ($F(3,63) = 16.33$, $p < 0.001$), where the direction of the COP displacement is clearly towards the side of the stimulation in the case of DC-GVS stimulations (Fig. 5 left panel). Tukey's HSD post hoc test confirmed that the lateral coronal displacement for DC-GVS left and right stimulations were significantly different than any other stimulations (Fig. 5, right panel). Figure 5 shows

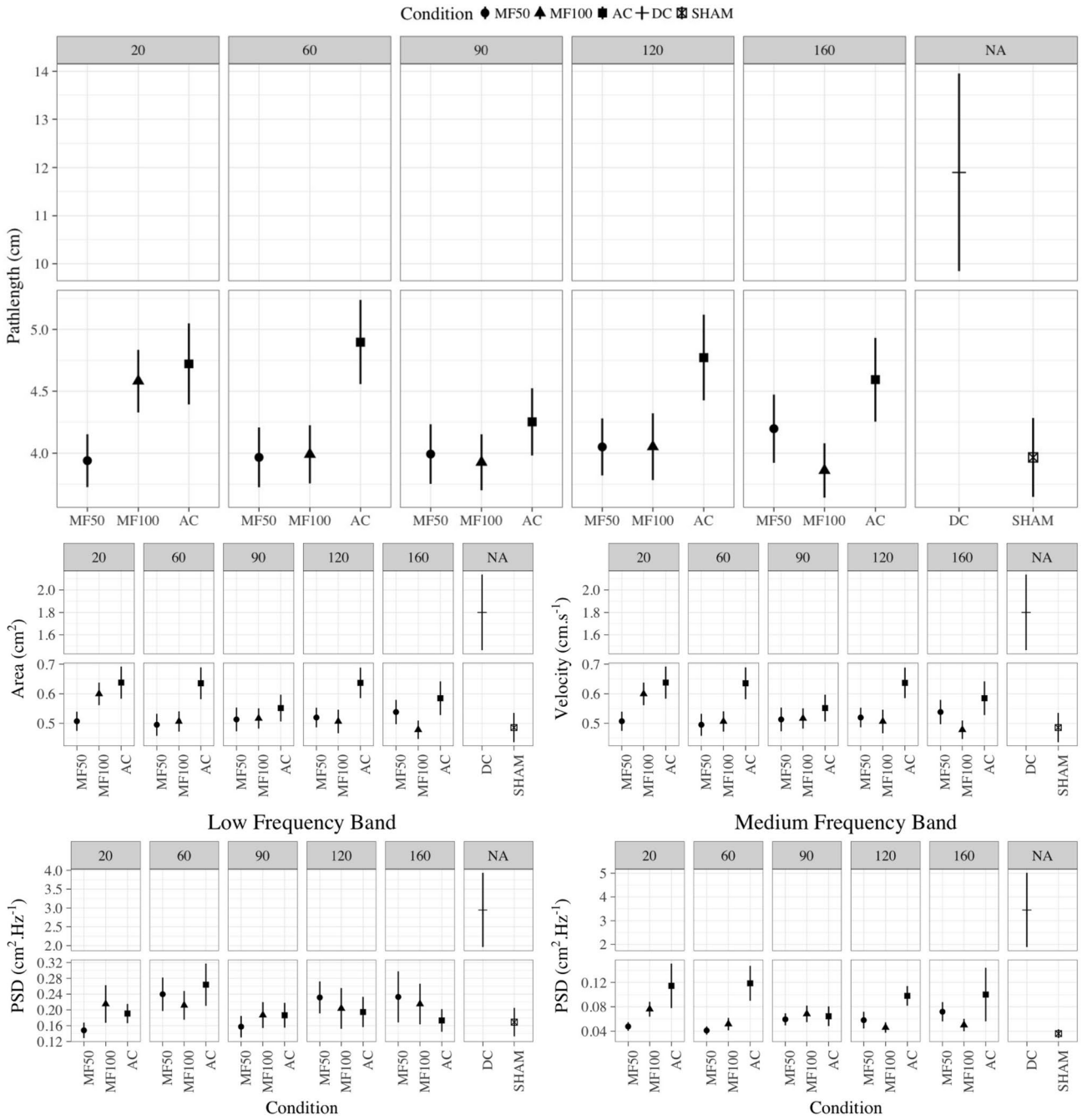

Fig. 4 Mean and standard error of the mean for each experimental condition in all conditions of frequency, for the pathlength (top panel), convex hull area (middle left panel), coronal velocity (middle right panel), power density for the low frequency band (bottom left panel) and power density for the medium frequency band. Only the DC-GVS shows significantly greater values than any other experimental conditions

that the DC-GVS anodal stimulation on the left side leads to an average maximum displacement to the left of − 1.59 (mean) ± 0.52 cm (standard error of mean) and an average displacement to the right for an anodal stimulation on the right of + 1.87 ± 0.40 cm.

No significant effects of side or side–exposure interactions were found for the other variables.

Finally, the three (exposure: AC-GVS, MF_{50mT} and MF_{100mT}) × 2 (side: left, right) × 5 (frequency: 20 Hz, 60 Hz, 90 Hz, 120 Hz and 160 Hz) within-subject ANOVA excluded both Sham and DC-GVS conditions to focus on time-varying signals and hence tested for frequency effects. Path length ($F(2,42) = 9.75$, $p < 0.001$), area ($F(2,42) = 4.52$, $p < 0.05$), and coronal velocity ($F(2,42) = 7.78$, $p < 0.01$)

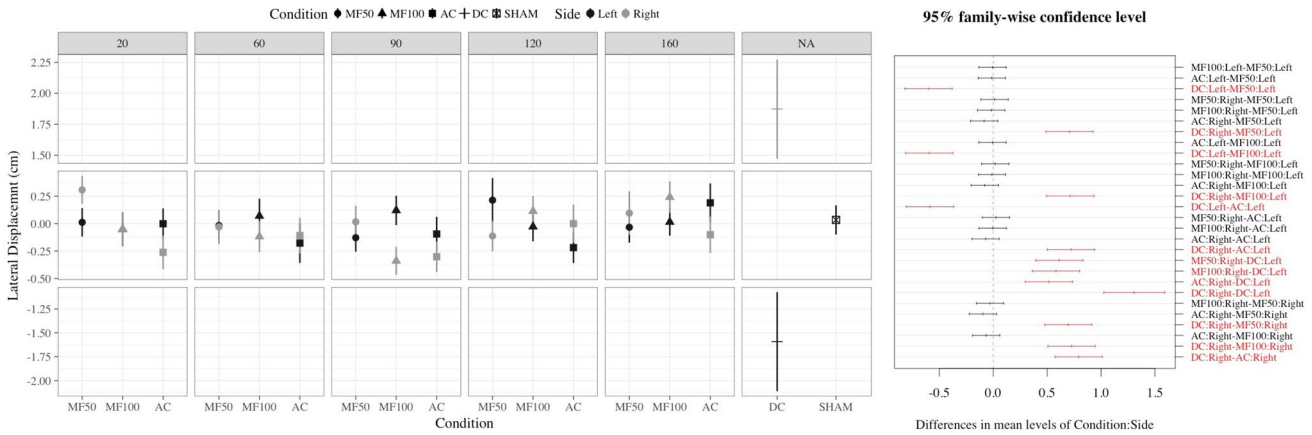

Fig. 5 Side effect for lateral coronal displacement. Positive values represent displacement towards the right side of the body. Negative values represent displacement towards the left side of the body. DC-GVS right exposure and left exposure lateral coronal displacements are significantly different from each other and from any other stimulations. The right panel represents the Tukey's HSD post hoc analysis comparing each condition to each other. Differences that do not include 0 (dotted line) are significant

showed a significant exposure on main effect between. Tukey's HSB revealed that for both path length and coronal velocity, the AC-GVS yielded higher values than the MF_{50mT} and MF_{100mT} conditions.

No frequency effects were found for any of the variables investigated in this study.

Head-mounted device stabilization effect

In a previous work, Day et al. (1997) presented maximum lateral displacement of the COP around 2 cm, while participants were standing with their feet together and were stimulated with a DC-GVS at 0.7 mA. In this work, we observed lateral displacement of the same order for a stimulation of 2 mA. Considering that many studies reported that DC-GVS effect is intensity-dependent (Fitzpatrick et al. 1994; Day et al. 1997; Zink et al. 1998), we were expecting a much larger effect on lateral displacement. Furthermore, the exposure apparatus used in this study is a unique, newly developed system with potential unexpected limitations. Therefore, it was decided to test for the effects of wearing the MF exposure device on standing balance (as opposed to standing without wearing the device). Consequently, path length, area, and coronal velocity were analyzed in 11 participants (4 males and 7 females, that did not participate in the actual experiment presented before), standing with their feet together and eyes closed on the force plate. The procedure consisted of two standing conditions with the MF exposure device placed on the head (inactive) and two with the device off the head. Figure 6 illustrates the results, showing significant lower values with the MF exposure device on head as compared to off head for path length ($F(1,10) = 24.56$, $p < 0.001$), Area ($F(1,10) = 21.19$, $p < 0.001$), and coronal velocity ($F(1,10) = 30.03$, $p < 0.001$). This is evidence of a significant stabilization effect resulting from wearing the exposure device, even though it is inactive.

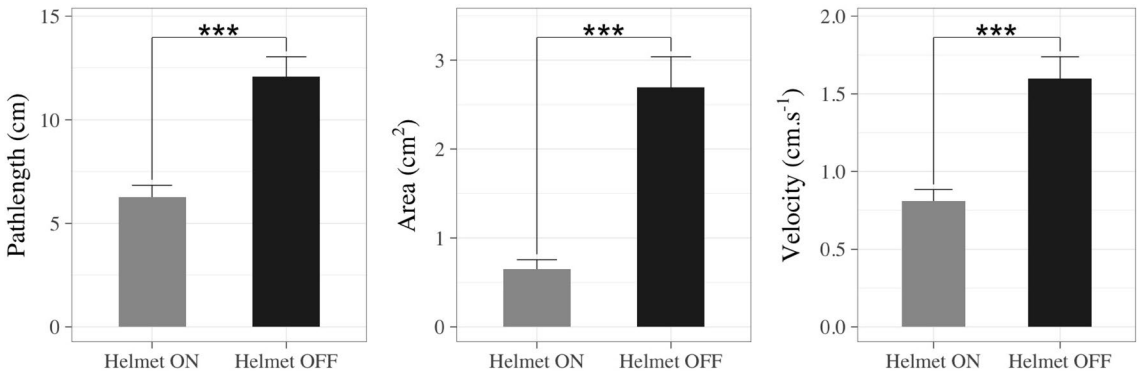

Fig. 6 The path length, the area and the coronal velocity are lower when with the exposure helmet on the head as compared to standing without it. The standing balance is reduced by half or more (i.e., stabilization effect) with the helmet on

Discussion

The main aim of this study was to explore the effects of a time-varying magnetic field exposure (including the power frequency) on human postural control. Since this effect is hypothesized to be mediated by the induced electric field in the vestibular system, AC electric stimulations (AC-GVS) were also studied. DC electric stimulation known as DC-GVS was used as a positive control.

The first important result was the confirmation that the positive control condition elicited the expected effects. Indeed, DC-GVS produced a de-stabilizing effect on the volunteers both in time domain characteristics (increased path length, area, coronal velocity) and frequency domain characteristics [increased absolute power density spectrum in both low frequency band (0–0.5 Hz) and medium frequency band (0.5–2 Hz)]. More importantly, this effect was confirmed as dependent on the side to which the stimulation occurred. These results were similar to previous findings of DC-GVS postural control modulations (Inglis et al. 1995; Fitzpatrick and Day 2004; Day and Guerraz 2007).

However, there were no significant differences between any of the electric and magnetic time-varying stimulations (AC-GVS at 1.5 mA, MFs at 50 mT and 100 mT) and the Sham exposure. This was unexpected since lower levels of magnetic flux densities are capable of inducing acute responses related to other neurophysiological processes: time-varying MFs between 20 and 50 Hz reliably produce magnetophosphenes at MF flux densities as low as 8–12 mT (Lövsund et al. 1980b). As mentioned earlier, magnetophosphenes are flickering white perceptions occurring in the dark with the eyes closed, due to the induction of E-fields and currents at the level of retinal rod cells, with perception thresholds corresponding to retinal current density estimated to be between 10 and 40 mA m^{-2} (Lövsund et al. 1980b; Attwell 2003; Hirata et al. 2011; Laakso and Hirata 2012, 2013) or an induced extracellular E-field in the retina of 0.01–0.06 V m^{-1} (Attwell 2003). Since retinal rod cells and vestibular hair cells both use graded potentials for signaling to afferent nerves, it was hypothesized that sufficient levels of MF exposure should induce electric fields capable of interacting with hair cells and thus possibly modulate postural control.

The first explanation for the lack of effect of time-varying exposures (AC or MF) in this study may result from failing to exceed an effect threshold. Based on available evidence from the literature, we expected that a 1.5 mA AC-GVS or 100 mT MF exposure would introduce a sufficiently high electric field that interacts with the vestibular system. DC stimulation of 1.5 mA is reported to interact with the vestibular system. For instance, Miranda et al. (2006) compared different montages of electrodes for a 2 mA transcranial DC stimulation: according to their calculations on a spherical model of the head, values between 80 and 100 mA m^{-2} could be reached at 5 cm under the anodal electrode. Similarly, Parazzini et al. (2011) assessed the maximum current density under the electrode of a 1 mA DC stimulation at 43 mA m^{-2}. Here, it can be assumed that current densities ranging from 40 to 80 mA m^{-2} were achieved in the vicinity of the vestibular system, which was enough to modulate vestibular function.

There is less literature regarding AC-GVS dosimetry, and none targeting the vestibular system specifically. A study by Laakso and Hirata (2013), however, reports current densities between 20 and 40 mA m^{-2} under the electrode for a 100 µA stimulation. To assess the order of magnitude of the current densities generated in our study, we assume a linear relationship between the applied current and their associated current densities produced. Therefore, values between 300 and 600 mA m^{-2} would most likely be reached at the mastoid level with a stimulus of 1.5 mA. Laakso and Hirata (2013) also showed that about 60% of the stimulation penetrated the skull within 5 cm from the center of the electrode, which, in our study would correspond to values in the range of 180–360 mA m^{-2} in the vicinity of the vestibular system.

With respect to electric fields, Laakso et al. (2015) showed a transcranial DC stimulation of 1 mA generates a maximum electric fields under the electrode at the cortex level ranging from 0.62 to 1.43 V m^{-1}. These values allow one to estimate that, under the same scenario, a 1.5 mA stimulation would produce E-fields between 1 and 2 V m^{-1}, which could be extrapolated to the location of the vestibular system in the current study.

This suggests the possibility that the lack of effect of the AC exposures on postural control may be related to the range of frequencies used. Therefore, in future studies, it might be more appropriate to investigate lower frequencies (1–10 Hz), which the vestibular system might be more sensitive to, as suggested by the findings of Hlavacka and Njiokiktjien (1985).

Regarding the time-varying MF conditions, the exposure level can be expressed as the time rate of change of the magnetic field, or dB/dt. Following the same steps presented in previous works (Valberg et al. 1997; Attwell 2003) we can provide a gross estimation of the electric field E produced at the level of the vestibular system. According to the Maxwell equations, $E = \frac{r}{2}\frac{\partial B}{\partial t} = \pi rfB$ where E is the induced electric field and r is the radius of the structure exposed and f the frequency of the stimulation. Then, for a vestibular system encapsulated in a 5-mm sphere, exposures of 50 mT (rms) and 100 mT (rms) at frequencies from 20 to 160 Hz have peak dB/dt between 8.9 T s^{-1} and 142 T s^{-1}, which we estimate corresponds roughly to peak-induced electric fields between

22.2 mV m^{-1} and 355 mV m^{-1}. These values exceed the 10 mV m^{-1} proposed by Attwell (2003) as an approximate magnetophosphene threshold.

Previous studies using weaker fields but longer exposure durations reported that ELF MFs may modulate postural stability, revealing an effect on standing balance (Thomas et al. 2001a, b; Legros et al. 2012). However, it is important to note that in the Legros et al.' study (2012) the exposure duration reached whole body flux densities between 0.2 mT and 1.8 mT for one hour as opposed to 5 s in the current work. It is possible that the effects reported in these studies are not only related to a vestibular modulation, but possibly at any level of the proprioceptive or the motor loops.

More importantly, the results from this study highlighted an important limitation that may have prevented potential effects to be observed: a strong stabilizing effect of the mechanical characteristics of the MF exposure device restricted the amplitude of the natural postural sway. This is a crucial result to be noted when interpreting observed results, as subtle exposure effects may not have been exhibited. Indeed, it is known that the effect of DC-GVS on postural performance is enhanced in less stable experimental conditions (Day and Guerraz 2007; Yang et al. 2015). More instability can be created by disabling the visual control (eyes closed), reducing proprioceptive input (foam pad underneath the feet) or reducing the distance between the feet to increase coronal sway (Day et al. 1993; McIlroy and Maki 1997). These factors have been controlled in this study, but they might have been counterbalanced by the stabilizing effect of the device delivering the MF stimulation coupled to the counterweight system.

The absence of effect reported in this work must therefore be considered carefully, recognizing that subtle effects may have been masked by the physical effect of the head device. As a consequence, other investigators conducting similar studies may choose to explore alternative methods. Also, considering more challenging conditions, maximizing the reliance on the vestibular system to maintain postural control might very well enhance the probability of detecting an effect.

Furthermore, postural control is not solely dependent on vestibular input, but rather a combination of visual input and other sensory input as well (Hansson et al. 2010), and even if postural control is a credible screening test for detecting imbalance, it provides nonspecific information regarding the exact origins of imbalance (Lang and McConn Walsh 2010). Therefore, by assessing other outcome measures, we may get a clearer view of the effects of time-varying MFs and AC-GVS exposure on the human vestibular system. Measurements such as the Subjective Visual Vertical, or exploration of nystagmus by recording eye movements during stimulation could be used to more specifically target vestibular functions (Lang and McConn Walsh 2010).

Acknowledgements The authors thank Mr. Lynn Keenliside for his technical assistance and Mr. Rob Kavet for his expertise and assistance in the revision of this manuscript. This project was supported by: Hydro-Québec (Canada) EDF-RTE (France), NationalGrid and Energy Network Association (UK), Electric Power Research Institute (EPRI–USA) and Lawson Internal Research funding. This work was also supported by MITACS through the MITACS-Accelerate Program. The funders had no role in study design, data collection and analysis, decision to publish, study approvals, or preparation of the manuscript.

References

Antunes A, Glover PM, Li Y et al (2012) Magnetic field effects on the vestibular system: calculation of the pressure on the cupula due to ionic current-induced Lorentz force. Phys Med Biol 57:4477–4487. https://doi.org/10.1088/0031-9155/57/14/4477

Attwell D (2003) Interaction of low frequency electric fields with the nervous system: the retina as a model system. Radiat Prot Dosimetry 106:341–348

Aw ST, Todd MJ, Aw GE et al (2008) Gentamicin vestibulotoxicity impairs human electrically evoked vestibulo-ocular reflex. Neurology 71:1776–1782. https://doi.org/10.1212/01.wnl.0000335971.43443.d9

Barlow HB, Kohn HI, Walsh EG (1947) Visual sensations aroused by magnetic fields. Am J Physiol 148:372

Bracken TD, Rankin RF, Senior RS et al (2001) Magnetic-field exposures of cable splicers in electrical network distribution vaults. Appl Occup Environ Hyg 16:369–379. https://doi.org/10.1080/10473220118938

Bronstein AM, Guerraz M (1999) Visual-vestibular control of posture and gait: physiological mechanisms and disorders. Curr Opin Neurol 12:5–11. https://doi.org/10.1097/00019052-199902000-00002

Carriot J, Jamali M, Chacron MJ, Cullen KE (2014) Statistics of the vestibular input experienced during natural self-motion: implications for neural processing. J Neurosci 34:8347–8357. https://doi.org/10.1523/JNEUROSCI.0692-14.2014

Cullen KE (2012) The vestibular system: multimodal integration and encoding of self-motion for motor control. Trends Neurosci 35:185–196. https://doi.org/10.1016/j.tins.2011.12.001

Curthoys IS, MacDougall HG (2012) What galvanic vestibular stimulation actually activates. Front Neurol 3:1–5. https://doi.org/10.3389/fneur.2012.00117

Curthoys IS, Grant JW, Burgess AM et al (2018) Otolithic receptor mechanisms for vestibular-evoked myogenic potentials: A review. Front Neurol 9:1–15. https://doi.org/10.3389/fneur.2018.00366

d'Arsonval A (1896) Dispositifs pour la mesure des courants alternatifs de toutes fréquences. Socicété Biol 450–451

Day BL, Guerraz M (2007) Feedforward versus feedback modulation of human vestibular-evoked balance responses by visual self-motion information. J Physiol 582:153–161. https://doi.org/10.1113/jphysiol.2007.132092

Day BL, Steiger MJ, Thompson PD, Marsden CD (1993) Effect of vision and stance width on human body motion when standing: implications for afferent control of lateral sway. J Physiol 469:479–499

Day BL, Séverac Cauquil A, Bartolomei L et al (1997) Human body-segment tilts induced by galvanic stimulation: a vestibularly driven balance protection mechanism. J Physiol 500(Pt 3):661–672. https://doi.org/10.1113/jphysiol.1997.sp022051

Eatock RA (2006) Vertebrate hair cells. Springer, New York

Fitzpatrick RC, Day BL (2004) Probing the human vestibular system with galvanic stimulation. J Appl Physiol 96:2301–2316. https://doi.org/10.1152/japplphysiol.00008.2004

Fitzpatrick R, Burke D, Gandevia SC (1994) Task-dependent reflex responses and movement illusions evoked by galvanic vestibular stimulation in standing humans. J Physiol 478 (Pt 2):363–372. https://doi.org/10.1113/jphysiol.1994.sp020257

Forbes PA, Dakin CJ, Vardy AN et al (2013) Frequency response of vestibular reflexes in neck, back, and lower limb muscles. J Neurophysiol 110:1869–1881. https://doi.org/10.1152/jn.00196.2013

Forbes PA, Siegmund GP, Schouten AC, Blouin J-S (2014) Task, muscle and frequency dependent vestibular control of posture. Front Integr Neurosci 8:94. https://doi.org/10.3389/fnint.2014.00094

Forbes PA, Luu BL, Van der Loos HFM et al (2016) Transformation of vestibular signals for the control of standing in humans. J Neurosci 36:11510–11520. https://doi.org/10.1523/JNEUROSCI.1902-16.2016

Forbes PA, Fice JB, Siegmund GP, Blouin JS (2018) Electrical vestibular stimuli evoke robust muscle activity in deep and superficial neck muscles in humans. Front Neurol 9:1–8. https://doi.org/10.3389/fneur.2018.00535

Foster KR (2003) Mechanisms of interaction of extremely low frequency electric fields and biological systems. Radiat Prot Dosimetry 106:301–310

Gensberger KD, Kaufmann A-K, Dietrich H et al (2016) Galvanic vestibular stimulation: cellular substrates and response patterns of neurons in the vestibulo-ocular network. J Neurosci 36:9097–9110. https://doi.org/10.1523/JNEUROSCI.4239-15.2016

Glover PM, Cavin I, Qian W et al (2007) Magnetic-field-induced vertigo: a theoretical and experimental investigation. Bioelectromagnetics 28:349–361. https://doi.org/10.1002/bem.20316

Glover PM, Li Y, Antunes A et al (2014) A dynamic model of the eye nystagmus response to high magnetic fields. Phys Med Biol 59:631–645. https://doi.org/10.1088/0031-9155/59/3/631

Goldberg JM, Smith CE, Fernández C (1984) Relation between discharge regularity and responses to externally applied galvanic currents in vestibular nerve afferents of the squirrel monkey. J Neurophysiol 51:1236–1256

Goldberg JM, Wilson VJ, Cullen KE, Angelaki DE, Broussard DM, Buttner-Ennever J, Fukushima K, Minor LB (2012) The vestibular system: a sixth sense. Oxford University Press, New York. https://doi.org/10.1093/acprof:oso/9780195167085.001.0001

Hansson EE, Beckman A, Håkansson A (2010) Effect of vision, proprioception, and the position of the vestibular organ on postural sway. Acta Otolaryngol 130:1358–1363. https://doi.org/10.3109/00016489.2010.498024

Hirata A, Takano Y, Fujiwara O et al (2011) An electric field induced in the retina and brain at threshold magnetic flux density causing magnetophosphenes. Phys Med Biol 56:4091–4101. https://doi.org/10.1088/0031-9155/56/13/022

Hlavacka F, Njiokiktjien C (1985) Postural responses evoked by sinusoidal galvanic stimulation of the labyrinth. Acta Otolaryngol 99:107–112

IEEE (2002) C95.6. IEEE standard for safety levels with respect to human exposure to electromagnetic fields, 0–3 kHz. The institute of Electrical and Electronics Engineers, Inc., New York

Inglis JT, Shupert CL, Hlavacka F, Horak FB (1995) Effect of galvanic vestibular stimulation on human postural responses during support surface translations. J Neurophysiol 73:896–901

International Commission on Non-Ionizing Radiation Protection (2010) Guidelines for limiting exposure to time-varying electric and magnetic fields (1 Hz to 100 kHz). Health Phys 99:818–836. https://doi.org/10.1097/HP.0b013e3181f06c86

Jefferys JGR, Deans J, Bikson M, Fox J (2003) Effects of weak electric fields on the activity of neurons and neuronal networks. Radiat Prot Dosimetry 106:321–323

Laakso I, Hirata A (2012) Computational analysis of thresholds for magnetophosphenes. Phys Med Biol 57:6147–6165. https://doi.org/10.1088/0031-9155/57/19/6147

Laakso I, Hirata A (2013) Computational analysis shows why transcranial alternating current stimulation induces retinal phosphenes. J Neural Eng 10:046009. https://doi.org/10.1088/1741-2560/10/4/046009

Laakso I, Tanaka S, Koyama S et al (2015) Inter-subject variability in electric fields of motor cortical tDCS. Brain Stimul 8:906–913. https://doi.org/10.1016/j.brs.2015.05.002

Lang EE, McConn Walsh R (2010) Vestibular function testing. Ir J Med Sci 179:173–178. https://doi.org/10.1007/s11845-010-0465-7

Legros A, Corbacio M, Beuter A et al (2012) Neurophysiological and behavioral effects of a 60 Hz, 1,800 μT magnetic field in humans. Eur J Appl Physiol 112:1751–1762. https://doi.org/10.1007/s00421-011-2130-x

Lövsund P, Öberg P, Nilsson SEG (1980a) Magneto- and electrophosphenes: a comparative study. Med Biol Eng Comput 18:758–764. https://doi.org/10.1007/BF02441902

Lövsund P, Öberg P, Nilsson SEG, Reuter T (1980b) Magnetophosphenes: a quantitative analysis of thresholds. Med Biol Eng Comput 18:326–334. https://doi.org/10.1007/BF02443387

Magnusson M, Enbom H, Johansson R, Wiklund J (1990) Significance of pressor input from the human feet in lateral postural control. The effect of hypothermia on galvanically induced body-sway. Acta Otolaryngol 110:321–327. https://doi.org/10.3109/00016489009107450

Marcelli V, Esposito F, Aragri A et al (2009) Spatio-temporal pattern of vestibular information processing after brief caloric stimulation. Eur J Radiol 70:312–316. https://doi.org/10.1016/j.ejrad.2008.01.042

McIlroy WE, Maki BE (1997) Preferred placement of the feet during quiet stance: development of a standardized foot placement for balance testing. Clin Biomech (Bristol Avon) 12:66–70

Mezei G, Bracken TD, Senior R, Kavet R (2006) Analyses of magnetic-field peak-exposure summary measures. J Expo Sci Environ Epidemiol 16:477–485. https://doi.org/10.1038/sj.jea.7500457

Miranda PC, Lomarev M, Hallett M (2006) Modeling the current distribution during transcranial direct current stimulation. Clin Neurophysiol 117:1623–1629. https://doi.org/10.1016/j.clinph.2006.04.009

Norris CH, Miller AJ, Perin P et al (1998) Mechanisms and effects of transepithelial polarization in the isolated semicircular canal. Hear Res 123:31–40. https://doi.org/10.1016/S0378-5955(98)00096-3

Otero-Millan J, Zee DS, Schubert MC et al (2017) Three-dimensional eye movement recordings during magnetic vestibular stimulation. J Neurol 264:7–12. https://doi.org/10.1007/s00415-017-8420-4

Paillard T, Noé F (2015) Techniques and methods for testing the postural function in healthy and pathological subjects. Biomed Res Int 2015:1–15. https://doi.org/10.1155/2015/891390

Parazzini M, Fiocchi S, Rossi E et al (2011) Transcranial direct current stimulation: estimation of the electric field and of the current density in an anatomical human head model. IEEE Trans Biomed Eng 58:1773–1780. https://doi.org/10.1109/TBME.2011.2116019

Prato FS, Thomas AW, Cook CM (2001) Human standing balance is affected by exposure to pulsed ELF magnetic fields: light intensity-dependent effects. Neuroreport 12:1501–1505. https://doi.org/10.1097/00001756-200105250-00040

R Core Team (2016) R: a language and environment for statistical computing. R Found. Stat. Comput. Vienna Austria 0:{ISBN} 3-900051-07-0

Rankin RF, Bracken TD, Senior RS et al (2002) Results of a multisite study of U.S. residential magnetic fields. J Expo Anal Environ Epidemiol 12:9–20. https://doi.org/10.1038/sj/jea/7500196

Roberts DC, Marcelli V, Gillen JS et al (2011) MRI magnetic field stimulates rotational sensors of the brain. Curr Biol 21:1635–1640. https://doi.org/10.1016/j.cub.2011.08.029

Saunders RD, Jefferys JGR (2002) Weak electric field interactions in the central nervous system. Health Phys 83:366–375

Saunders RD, Jefferys JGR (2007) A neurobiological basis for ELF guidelines. Health Phys 92:596–603. https://doi.org/10.1097/01.HP.0000257856.83294.3e

Stål F, Fransson P, Magnusson M, Karlberg M (2003) Effects of hypothermic anesthesia of the feet on vibration-induced body sway and adaptation. J Vestib Res 13:39–52

Thomas AW, Drost DJ, Prato FS (2001a) Human subjects exposed to a specific pulsed (200 microT) magnetic field: effects on normal standing balance. Neurosci Lett 297:121–124

Thomas AW, White KP, Drost DJ et al (2001b) A comparison of rheumatoid arthritis and fibromyalgia patients and healthy controls exposed to a pulsed (200 microT) magnetic field: effects on normal standing balance. Neurosci Lett 309:17–20

Tinsley JN, Molodtsov MI, Prevedel R et al (2016) Direct detection of a single photon by humans. Nat Commun 7:12172. https://doi.org/10.1038/ncomms12172

Valberg P, Kavet R, Rafferty CN (1997) Can Low-Level 50/60 Hz Electric and Magnetic Fields Cause Biological Effects? Radiat Res 148:2. https://doi.org/10.2307/3579533

van Nierop LE (2015) The magnetized brain: working mechanisms for the effects of MRI-related magnetic fields on cognition, postural stability, and oculomotor function. Utrecht, Netherlands

van Nierop LE, Slottje P, Kingma H, Kromhout H (2013) MRI-related static magnetic stray fields and postural body sway: A double-blind randomized crossover study. Magn Reson Med 70:232–240. https://doi.org/10.1002/mrm.24454

Ward BK, Roberts DC, Della Santina CC et al (2015) Vestibular stimulation by magnetic fields. Ann N Y Acad Sci 1343:69–79. https://doi.org/10.1111/nyas.12702

World Health Organization (2007) Environmental health criteria 238 extremely low frequency fields. World Health Organization, Geneva, p 543

Yang Y, Pu F, Lv X et al (2015) Comparison of postural responses to galvanic vestibular stimulation between pilots and the general populace. Biomed Res Int. https://doi.org/10.1155/2015/567690

Zink R, Bucher SF, Weiss A et al (1998) Effects of galvanic vestibular stimulation on otolithic and semicircular canal eye movements and perceived vertical. Electroencephalogr Clin Neurophysiol 107:200–205. https://doi.org/10.1016/S0013-4694(98)00056-X